Experimental analysis of masonry ring beams reinforced with composite materials

A. Borri & R. Sisti
University of Perugia, Perugia, Italy
M. Corradi
Northumbria University, Newcastle Upon Tyne, UK & University of Perugia, Perugia, Italy
A. Giannantoni
Self-employed engineer, Perugia, Italy

ABSTRACT: It is known that the application of a ring beam is an effective method to prevent an out-of-plane collapse mechanism of perimeter wall panels. However this effective reinforcing method presents some problems. In order to address this, this paper describes the problems associated with this reinforcing method and studies a new technique for reinforcing historic masonry buildings by realizing a new type of ring beam made of recycled old stones or bricks reinforced at the bed joints with glass-fibre sheets, GFRP (Glass Fiber Reinforced Polymer) grids or/and PBO (polybenzoxazole: poly-p-phenylene benzobisoxazole) cords. An experimental investigation has been carried out on 8 full-scale rubble-stone or brickwork masonry ring beams tested in bending. The testing included the use of composite materials inserted into the mortar joints during the fabrication phase of the beams and pinned end conditions (four-point bending configuration). Beams were reinforced with different reinforcement layout.

1 INTRODUCION

Historical masonry constructions tend to lack connections between walls and between walls and floors. In order to achieve unitary behaviour of the structure against earthquakes, masonry structures must be upgraded so that they avoid local collapse and have integrating structural elements.

Figure 1. Example of a RC ring-beam.

In the past, improvement has been achieved by tie rod or ring beams and, in older buildings, it is possible to observe wooden ties and connectors inside masonry. In recent years wood ring beams have been replaced with RC (Reinforced Concrete) ring beam (Fig. 1) (Penazzi et al. 2001, D'Ayala et al. 2003, Alexandris et al. 2004); however recent earthquakes have shown the limitations of the later technique which prove to be ineffective when in-adequately designed, when not well connected to the existing masonry below, when built above poor masonry or when attached to a heavy floor.

It has been recognized by now that the greater stiffness of the RC ring beam compared to the stiffness of the masonry, produces a different response in these two materials during earthquakes and causes the load to be unevenly spread. In order to prevent out-of-plane collapse mechanisms, the action of vertical static loads may contribute to stabilize wall panels, but the application of stiff RC ring beam may cause the re-distribution of vertical compressive stresses and some portions of masonry could results unloaded and, during earthquakes, be prone to become unstable (Fig. 2) (Binda et al. 1999, Furukawa 2009, Magenes at al. 2014).

Figure 2. Example of an out-of-plane collapse due to poor connection between the RC ring beam and the underlying masonry.

Nowadays, it's usual to apply steel-profiles or masonry ring beams (Figs. 3-4). However, when a building is faced with stone, the ring beams are made thinner than the wall so that they are screened

and remain invisible on the façade. This kind of reinforcement is impossible when the thickness of the wall is very small. The behavior and the mechanical properties of RC is also very different compared to masonry.

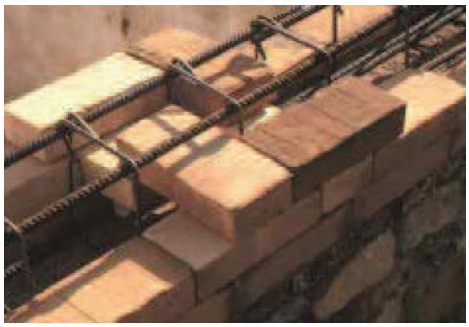

Figure 3. Example of a brickwork steel-reinforced ring-beam.

Figure 4. Example of a steel-profile ring-beam.

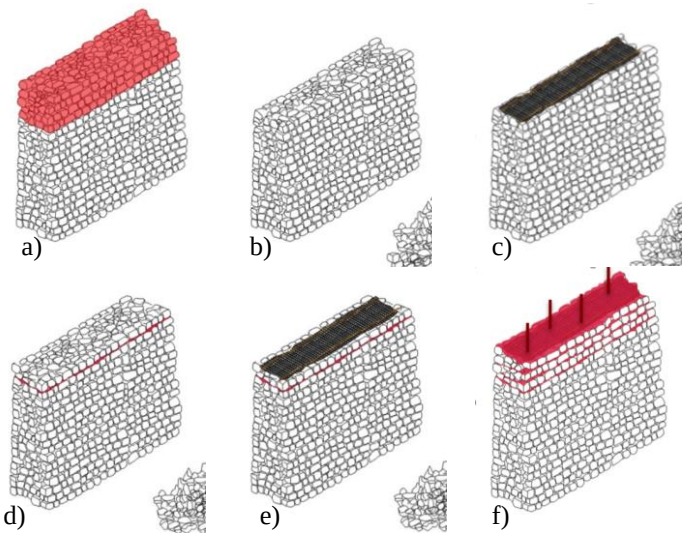

Figure 5. Construction methods of a reinforced masonry ring beam: a-b) taking down the upper part of the wall; c) laying out the first mortar bed reinforced with the composite; d) laying the stones; e) spreading the second layer of reinforced mortar; f) repeating the phases d)-e) until reaching the required height.

Recently researchers have focused their interest on the use of composite materials coupled with non-polymeric matrixes, like lime-based mortars (Huang et al. 2005, Prota et al. 2006, Corradi et al. 2008, Papanicolaou et al. 2008, Gattesco and Dudine 2010, Castori et al. 2015, Borri et al. 2015). The aim is to avoid the use of epoxy or other polymeric resins, due to their critical long-term behavior. In this area, the new reinforced masonry ring beam proposed in this paper is based on the aspiration to use existing materials, reinforced inside the mortar joints with composites. The system involves taking down a small portion of the upper part of perimeter walls and later rebuilding them, alternating recovered stones and hydraulics mortar bed with tensile resistant composite materials inside, like GFRP sheets and grids (Fig. 5). Both have been extensively used in the past to strengthen wall panels, vaults and arches (Tumilian et al. 2001, Roca et al. 2010, Borri et al. 2014, Corradi et al. 2014).

As solid brick or ashlar stone masonry, characterized by both regular horizontal and staggered vertical joints, can deal with horizontal tensile loads thanks to the friction in the horizontal bed joints (Fig. 6), whereas random rubble stone masonry relies only on the cohesion of mortar. For that reason, in the past centuries, this kind of masonry was reinforced by inserting wooden beams inside masonry during its construction in order to bind the elements to each other and create a “pseudo-tensile” strength, as defined by Giuffrè (Giuffrè 1995). The resistance of these elements to sliding is due to the winding shape of the beams rather than the adhesion between wood and mortar, and for this reason the resistance is nondependent of the compression stress in the masonry.

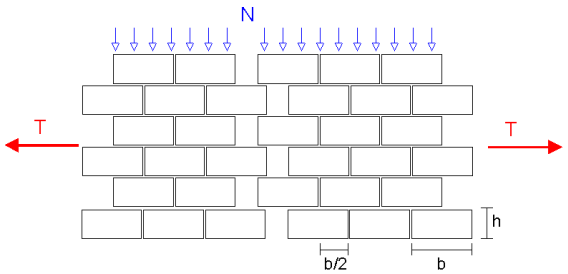

Figure 6. The response of a wall with regular horizontal bed mortar joints to horizontal tensile loading (Cangi, 2012).

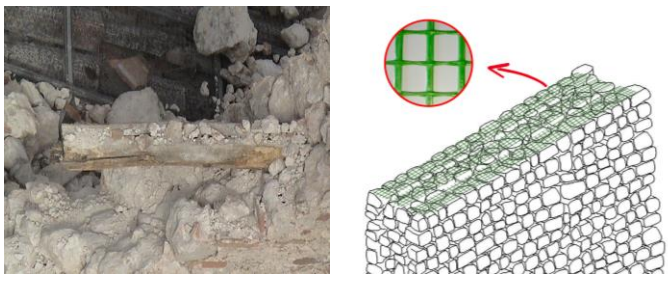

(a) (b)

Figure 7. (a) Example of how a wooden beam is inserted inside masonry in an old building damaged by the L’Aquila earthquake in 2009; (b) Example of application of a GFRP grid.

The system proposed in this paper is inspired by the technique mentioned above: the wooden beams were replaced with nets or grids in composite material (Fig. 7). In previous studies we proposed a system obtained by overlapping different layers of bricks and glass (Borri et al. 2004) or steel cords

(Borri et at. 2009) embedded within a cementitious grout.

2 EXPERIMENTAL WORK

2.1 *Description of specimens*

Ten masonry beams were constructed and subjected to bending test, in a vertical and horizontal plane.

Eight samples were made of stone masonry and had a length of 5 m and a cross-section of 0.5 x 0.5 m. They were formed by 3 layers of stone and mortar and 4 layers of reinforcement. They were built with a ready-to-use hydraulic lime-mortar (denomination: CM50).

In order to evaluate different kinds of reinforcement, various materials were inserted into the horizontal bed joints. Two beams were strengthened with a glass fiber mesh sheet of the same width as the specimen and twisted PBO (1,4-benzene dicarboxylic acid, polymer with 4,6-diamino-1, 3- benzenediol dihydrochloride) cords were added at the lateral far ends of the mesh (Figs. 8, 9a).

The third and fourth specimens differed from earlier ones in the configuration of PBO cords. In this case ropes were used ropes with-in a unidirectional core of PBO fiber and a protection cover of PET (polyethylene terephthalate) (Fig. 9b).

Four stone beams were built inserting a GFRP grid, made of AR (Alkali-Resistant) glass fiber with zirconium content equal to or over 16%, and of thermosetting epoxy vinyl ester resin. A rigid square meshes sized 33x33 mm were used in samples P5 and P6, whereas dimensions of 66x66 mm were employed in the P7 and P8 samples (Fig. 10).

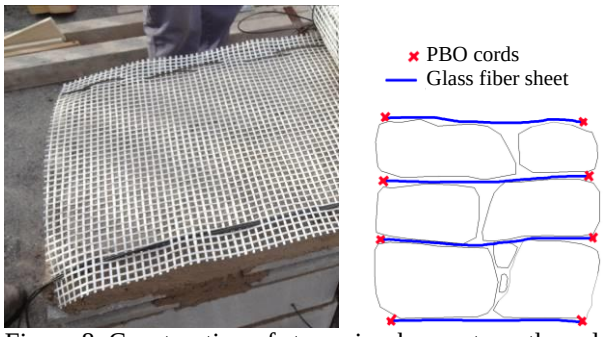

Figure 8. Construction of stone ring-beam strengthened with glass fiber sheets and PBO cords.


(a)

(b)

Figure 9. The cords used to reinforce the samples: (a) twisted PBO cord, (b) PBO cord with unidirectional core.

The remaining two samples were made of brickwork masonry. Their length were the same as the other specimens (5 m) whereas the cross-section was 0.4 x 0.33 m and they were formed by 4 courses of bricks and mortar and 5 layers of reinforcement (Fig. 11). The mortar used in their construction was a ready-to-use cement-based mortar (denomination: M15).

Figure 10. Construction of stone ring-beam strengthened with GFRP grids.

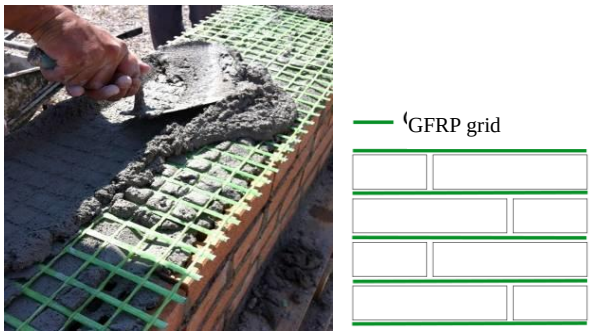

Figure 11. Construction of brickwork ring-beam using a GFRP grid.

Each test is identified with a code of three indices, the first of which indicates the masonry type and the progressive number identifying the panel (P = stone-masonry, L = brick-masonry), the second the type of strengthening (T = glass fiber sheet and PBO cord with twisted configuration, U = glass fiber mesh and PBO cord with unidirectional core, G33 = GFRP grid with a mesh size of 33 x 33 mm; G66 = GFRP grid with a mesh size of of 66 x 66 mm) and lastly the third the plane of loading (V = vertical, H = horizontal).

During the construction, the specimens were supported by wooden scaffoldings which were removed before the tests. The ends of the beams were rested on concrete blocks for 0.5 m, so the span is 4.0 m.

2.2 *Material characterization*

2.2.1 *Mortars*

The strength of the two mortars (CM50 and M15) was determined by compression tests on cylindrical samples approx. 95 mm in diameter and approx. 190 mm in height according to UNI EN 12390-3. The re-

sults are reported in Table 1 as a mean of three specimens for each beam.

The samples were from P3 and P4 beams showed lower strength due to a shorter and worse ripening.

Table 1. Properties of mortars.

	Weight density [kN/m^3]	Compressive strength		
		Mean [MPa]	sample size	CoV [%]
CM50_P1	19.84	7.35	3	7.30
CM50_P2	19.88	6.96	3	14.36
CM50_P3	18.13	3.82	3	7.64
CM50_P4	18.35	3.76	3	17.11
CM50_P5	18.10	6.57	3	7.83
CM50_P8	18.81	37.48	3	3.13
M15_L9	20.23	10.65	3	7.70
M15_L10	20.10	10.56	3	4.94

CoV=Coefficient of Variation

2.2.2 *Stones*

The stones from which the beams were made are from an old building seriously damaged by the L'Aquila earthquake in 2009.

Standard test specification UNI EN 1926 was used to find compressive strength, the results of which are listed in Table 2.

Table 2. Properties of stones.

	Sample dimensions [mm]	Weight density [kN/m^3]	Failure load [kN]	Compression strength [MPa]
S1	54.6x55.3x67.1	24.87	74.80	24.77
S2	50.4x40.7x68.7	24.04	73.61	21.29
S3	56.8x49.4x69.9	25.98	73.77	26.31
S4	55.7x69.1x70.9	25.92	97.34	25.33
	mean	25.20	-	24.42
	CoV			8.94 %

CoV=Coefficient of Variation

2.2.3 *Bricks*

The brick units used in L9 and L10 beams were hollow clay bricks of 55 x 120 x 250 mm, with 36% of void area.

Compression tests were performed on five bricks in the direction parallel to the holes and they showed a compressive strength of 46.33 MPa; while a strength of 11.53 MPa was obtained from the four tests carried out in the in the perpendicular direction.

2.2.4 *PBO cords*

The cords used to reinforced the first four samples were made of PBO fibers, commercially known as Zylon and produced and commercialized by Toyobo. This material was selected for his high Young's modulus and tensile strength, for the good resistance to creep and for the great flexibility.

Two kind of cords have been used as reinforcement: types T, with a twisted configuration, and U, with a unidirectional fiber core.

Table 3 summarizes the results obtained from tensile tests carried out in accordance with procedures established by ASTM D2256.

The tensile strengths of the two types of cord are similar whereas the Young's modulus of U cords are higher than the T ones. If the behavior is supposed linear until the failure, the elongations at failure are respectively 1.07% for the U cords and 3.22% for the T cords.

Table 3. Mechanical properties of PBO cords.

		T cords	U cords
Nominal diameter	[mm]	4	4
Rope configuration		twisted	unidirectional
Sample size		6	9
Failure tensile load (mean)	[kN]	12.25	11.19
Tensile strength (mean)	[MPa]	2923	2661
Young's modulus (mean)	[GPa]	91	250

2.2.5 *GFRP grid*

Both glass-based composites used in this experimental campaign are produced by Fibre Net S.r.l using AR-glass (Alkali-Resistant).

The glass fiber sheet (FBGR 220-12) is made of a square mesh with nominal dimensions of 12x12 mm. In both direction there are 0.48 mm^2 of fiber per cm of width and the failure load is 70 kN/m.

The GFRP grid is made up of alkali resistant glass fiber pre-impregnated with thermosetting epoxy vinyl ester resin. The grid is characterized by square mesh with nominal dimensions of 66 x 66 mm or 33 x 33 mm and the weaving is with multiple twisted warp and flat weft embedded between warp yarns. Specimens of multiple twisted warp and weft direction were extracted and mechanical characteristics were analyzed via tensile tests and are shown in Table 4.

Table 4. Mechanical properties of GFRP grid.

		Warp	Weft
Tensile strength	[MPa]	634	558
Sample size	[-]	15	13
Cross section	[mm^2]	7.13	8.52
Elongation at failure	[%]	1.60	1.56
Young modulus	[GPa]	39.63	35.72

2.3 *Test procedure*

In this paper only the first results from 8 tests are reported. The beams were simply supported at ends with four meters of span (L) and the load was uniformly distributed along the two central meters (Fig. 12).

Linear Variable Differential Transducers (LVDTs) were placed at ¼ , ½ and ¾ of beam's span (4 m) to register vertical deflections. When cracks appeared just for the weight of the beam it-

self, the displacements were measured manually with a millimetric sensitivity of measurements.

In order to bend the beams in their horizontal plane and simulate the seismic action, some specimens were confined with wooden planks and webbings clamped with ratchets and then were rotated 90° (Fig. 13). After this rotation the load was spread on the upper surface.

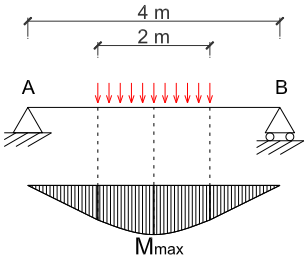

Figure 12. Arrangement of bending test with bending moment diagram (beam span L=4 m).

Figure 13. Rotation of a beam which were tested in horizontal plane.

2.4 *Results*

Results of all tests are presented in Table 5. In this table maximum mid-span moments produced by self-weight (M_w) and by external load (M_{Load}) are listed.

With regard to the specimens reinforced using PBO cords and glass-fibre sheets, the P1-T-V sample was bended in vertical plane and the load was applied in step of 0.1 kN, stacking cement bags. When a 16 kN-load was put over the beam, suddenly two vertical cracks formed, far from the rests 1.97 and 2.22 m, and the specimen leaned on the ground.

In P2-T-H, P3-U-V and P4-UH specimens, one or two cracks appeared in the middle part of the ring-beams as result of self-weight loads when the wooden scaffoldings were dismantled. Looking into the cracks, it could be observed the breaking of the glass fiber sheet, whereas the PBO cords were not damaged (Fig. 14a). The cracking also indicate the transition from an elastic behavior (in which all the reinforcing materials collaborate) to a plastic one (in which just the PBO cords provided the tensile strength). After the failure of the glass-fibre sheet, the load was applied in order to analyze the beam's plastic behavior. In all the three cases the deflection of the beam increased considerably until it leaned on ground; however the failure of PBO cords was never reached (Fig. 14b).

The different behavior between P1-T-V and P3-U-V test (both loaded in vertical plane, similar reinforcement arrangement) might have been influenced by the different mortar compressive strength (Tab. 1). For P1-T-V sample twisted PBO cords were used while unidirectional ones were adopted in P3-U-V. It should be also pointed out that P3-U-V was cured for a shorter period of time (84 days instead of 145). The different configuration of the PBO cords may have affected the response: the rougher surface of the twisted cords used in P1-T-V test may have favored the adhesion with the matrix compared to that which is developed with the smother protection cover of the other kind of cords.

The other specimens did not exhibit any crack during the loading phase.

(a) (b)

Figure 14. (a) Crack pattern produced by gravity self-weight load. (b) Ring-beam No. P3-U-V after testing.

The 8 simply-supported specimens that had failure initiating at mid-span had similar longitudinal and transverse strain gradients prior to failure.

With regard to the specimens reinforced using GFRP grids, the overall capacity of the ring-beams was significantly higher compare the one measured for specimens reinforced with PBO cords and glass-fibre sheets. For a load of 21 kN, specimen P5-G33-V exhibited vertical cracks on both the lateral vertical surfaces. By increasing the load magnitude, the ring beam underwent a progressive degradation: the number of vertical cracks amplified and horizontal crack at the bed joints opened near the beam's ends (Fig. 15). At beam's mid-span, diagonal cracks also opened and composite partially separated from the mortar. The capacity of the beam was 56.8 kN.

Specimen P8-G66-H exhibits vertical cracks at mid-span for a load of 10.5 kN. The maximum load applied on this ring-beam was 43.1 kN. For this load level many vertical cracks opened at beam intrados (Fig. 16). However it was not possible to take the specimen to failure for the difficulty in the application of the external load.

With regard to specimen L9-G33-V, for a load level of 14.6 kN, several vertical cracks opened at mid-span. By increasing the magnitude of the vertical load, cracks spread toward beam extrados.

Again, composite detached from the its matrix (the mortar) at the joint between the first/second and second/third course of bricks (Fig. 17).

Figure 15. Ring beam No. P5-G33-V.

Figure 16. Test No. P8-G66-H.

Figure 17. Test No. L9-G33-V

Figure 18. Test No. L10_G33_H

For L10-G33-H specimen, the maximum external load applied was 38.3 kN. Test was stopped at this level of load without having reached the failure of the masonry beam (Fig. 18).

For all bending tests conducted, diagrams of vertical deflections vs. position have been plotted in such a way that it is possible to appreciate the deformed configuration of the masonry beam. Figure 19 shows these curves at different load levels for beam L10-G33-H.

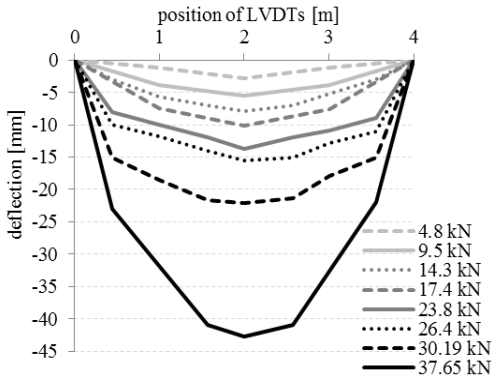

Figure 19. Deflection vs. position for different load values (L10_G33_H).

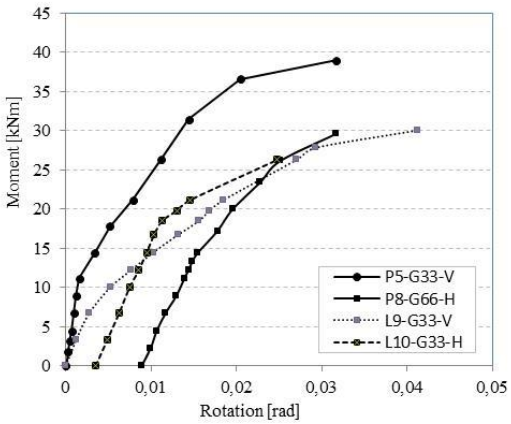

Figure 20. Moment curvature response.

Table 5. Results of bending tests.

	Specific weight [kN/m^3]	**M_w [kNm]**	**Max Load [kN]**	**M_{Load} [kNm]**	**M_{TOT} [kNm]**
P1-T-V	21.4	10.7	16.0	11.77	22.47
P2-T-H	21.4	10.7	9.0	6.62	17.32
P3-U-V	21.4	10.7	18.0	13.24	23.94
P4-U-H	21.4	10.7	16.0	11.77	22.47
P5-G33-V	21.4	10.7	56.8	38.99	49.69
P8-G66-H	21.4	10.7	43.1	29.57	40.27
L9-G33-V	14.64	3.86	51.2	35.19	39.05
L10-G33-H	14.64	3.86	38.3*	26.29	30.15

*Maximum load applied (without beam failure). M_w= Maximum mid-span bending moment produced by self-weight, M_{Load}= Maximum mid-span moment produced by external load; M_{Tot}= M_w+M_{Load}.

Figure 20 shows the moment-curvature response. The calculation of the bending moments in loaded ring-beam was made by considering the applied external load and neglecting the contribution of the self-weight. The curvature is expressed in terms of beam rotation at the ends. Figure 20 only shows the last cycle of loading: tests No. L10-G33-H and P6-G66-H present a residual deformation produced during the previous loading phase.

Following the bending test on specimen P1-T-V, an undamaged portion of this beam was tested in compression in order to determine the compressive strength of stone masonry.

The load was generated by means of two 1000 kN hydraulic jacks (reacting against a closed steel frame), distributed to an area of 0.5 x 0.5 m through a steel plate. On the lateral surfaces three LVDTs were set to measure the displacement occurred.

A compressive strength of 3.63 MPa and a secant elasticity modulus of 4458 MPa were measured, where the Young's modulus was calculate using two points located along the stress-strain curve at 10% and 40% of the maximum compressive stress.
The test was stopped because of the maximum load carrying capacity of steel frame was reached, even if the masonry had a compressive strain of approx. 2.3‰. Figure 21 shows that the actual curve could be reasonably well approximated to an ideal elastic-plastic model with ultimate deformation of 3.5‰.

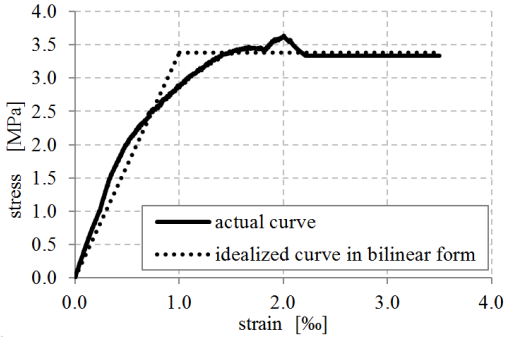

Figure 21. Behavior of stone masonry obtained from compressive tests.

3 COMPARISON BETWEEN ANALYTICAL PREDICTION AND TESTS RESULTS

A simplified method, based on basic beam bending theory, was examined to determine the accuracy with which they estimated the mid-span moment at failure for a given test. The ultimate bending moment capacity of each beam was calculated on the basis of the following hypothesis: linear strain diagram (plane cross section remaining plane after the deformations); perfect bond between masonry and reinforcing materials; negligible tensile strength of masonry, reinforcing materials nonreactive in compression.

The stress-strain relationships of stone masonry is assumed to be identical to the bilinear curve obtained from the compression test; while a compressive strength of brick masonry of 11.04 MPa was evaluated according to Italian code and a bilinear behavior was adopted with a Young's modulus of 11040 MPa.

Maximum mid-span moment values calculated using the analytical method and compared with experimental results are summarized for all the beam tests in Table 7. We can see in this table that there is good agreement between the analytical calculations and experimental results in terms of maximum bending moment. However for the first four tests, results diverge: this is probably due to the fact that the stress induced by the beam's self-weight caused the failure of both the glass fibre and of the bonding between the fibre and the mortar and this partially compromised the beam bending capacity. By increasing the bending load, only the PBO cords effectively acted to resist. Analytical value has been calculated by considering both glass fibre and PBO cord contribution and this caused an overestimation of the beam capacity.

Table 6. Beam capacity in terms of bending strength: experimental vs. numerical.

	M_{cal} [kNm]	M_{exp} [kNm]	M_{cal}/M_{exp} [%]
P1-T-V	41.49	22.47	84.6
P2-T-H	36.27	17.32	109.4
P3-U-V	43.57	23.94	82.0
P4-U-H	32.42	22.47	44.3
P5-G33-V	46.14	49.69	-7.1
P8-G66-H	38.75	40.27	7.7
L9-G33-V	49.31	39.05	-4.4
L10-G33-H	43.36	30.15*	10.3

4 CONCLUSIONS

A series of tests of composite material-reinforced masonry ring-beams were experimentally examined at the University of Perugia (Italy) Structural Testing Laboratory to help develop estimates of their flexural capacity in both vertical and horizontal planes. Two different materials (stones and bricks) and three types of fibres (glass-fibre sheet, GFRP grid and PBO cord) were examined and used as reinforcement. All specimens were tested in four point bend with simply-supported end conditions.

The method consists in the construction of a new stone- or brick-masonry ring beam at the roof level of the building using recycled stones/bricks. This reinforcement method allows to keep the masonry fair faced appearance. Reinforcement is completely embedded into the horizontal mortar joints.

Mid-span maximum moments at failure were estimated using linear methods based on basic beam theory. Examining the calculated moment magnitudes, findings from the study indicated that:

1) Four tests have been carried out on stone beams reinforced using GFRP grids and PBO cords. Results demonstrated that the reinforced beams are able to resist high bending loads only after the self-weight caused the opening of initial cracks in the mortar joints.

2) During the tests, the PBO cords never failed in tension, but by increasing the external bending load, vertical deflections and crack widths became very large. The bonding between the PBO cord and its matrix (the mortar) was poor and this partially compromised the resisting action of the PBO cords. Only when the vertical deflections and deformations of the ring-beam reached high levels, the contribution of PBO cords was activated.

3) Reinforcement was more effective when GFRP grids were used (tests P5, P8, L9 and L10). Results of the last four flexure tests evidenced high values in terms of capacity loads and bonding characteristics between GFRP and mortar. For these tests, the analytical calculations of the maximum bending moment was in good agreement with experimental findings.

4) For beams reinforced with GFRP grids, the bending capacity was very high for all tests performed in both vertical and horizontal planes.

5 ACKNOWLEDGEMENTS

The authors express their gratitude to Tecnoclima Group s.r.l. for manufacturing facilities provided. This project was partial sponsored by the Italian Ministry of Education [ReLUIS (2014) Linea di ricerca WP1 e WP2]. The authors acknowledge Fibre Net S.r.l. for providing the composite materials.The authors also thank Mr. Alessio Molinari, Mr. Mattia Procacci, Mrs. Ilenia Rinchi and Mr. Alessio Di Mauro.

6 REFERENCES

Alexandris, A., Protopapa, E. & Psycharis, I. 2004. Collapse mechanisms of masonry buildings derived by the distinct element method. In *Proceedings of the 13th world conference on earthquake engineering*.

ASTM D2256 2002. Standard test method for tensile properties of yarns by the single-strand method.

Binda, L., Gambarotta, L., Lagomarsino, S. & Modena, C. 1999. A multilevel approach to the damage assessment and seismic improvement of masonry buildings in Italy. *Seismic damage to masonry buildings*. Balkema, Rotterdam, 170-195.

Borri, A., Castori, G. & Grazini, A. 2009. Retrofitting of masonry building with reinforced masonry ring-beam. *Construction and Building Materials* 23(5): 1892-1901.

Borri, A., Castori, G., Corradi, M. & Sisti, R. 2014. Masonry wall panels with GFRP and steel-cord strengthening subjected to cyclic shear: An experimental study. *Construction and Building Materials* 56:63-73.

Borri, A., Corradi, M., Sisti, R., Buratti, C., Belloni, E. & Moretti, E. 2015. Masonry wall panels retrofitted with thermal-insulating GFRP-reinforced jacketing. *Materials and Structures*.

Cangi, G. 2012. *Manuale del recupero strutturale e antisismico*. [in Italian] Ed. DEI, Rome.

Castori, G., Borri, A. & Corradi, M. 2015. Behavior of thin masonry arches repaired using composite materials. *Journal of Composites, part B*.

Corradi, M., Borri, A. & Vignoli, A. 2008. Experimental evaluation of the in-plane shear behaviour of masonry walls retrofitted using conventional and innovative methods. *Masonry International* 21(1): 29-42.

Corradi, M., Borri, A., Castori, G. & Sisti, R. 2014. Shear strengthening of wall panels through jacketing with cement mortar reinforced by GFRP grids. *Composites Part B: Engineering* 64: 33-42.

D'Ayala, D. & Speranza, E. 2003. Definition of collapse mechanisms and seismic vulnerability of historic masonry buildings. *Earthquake Spectra* 19(3): 479-509.

Frumento, S., Giovinazzi, S., Lagomarsino, S. & Podestà, S. 2006. Seismic retrofitting of unreinforced masonry buildings in Italy.

Furukawa, A. & Ohta, Y. 2009. Failure process of masonry buildings during earthquake and associated casualty risk evaluation. *Natural hazards* 49(1), 25-51.

Gattesco, N. & Dudine, A. 2010. Effectiveness of masonry strengthening technique made with a plaster reinforced with a GFRP net. In *Proc. 8th International Masonry Conference* 5-9 July 2010, Dresden, Germany.

Giuffrè, A. 1995. Seismic damage in historic town centres and attenuation criteria.

Huang, X., Birman, V., Nanni, A. & Tunis, G. 2005. Properties and potential for application of steel reinforced polymer and steel reinforced grout composites. *Compos: Part B* 36:73–82.

Javed, M., Naeem, A., Penna, A. & Magenes, G. 2005. Behavior of masonry structures during the Kashmir 2005 earthquake. In *Proc. Of the First European Conference on Earthquake Engineering and Seismology*, Geneva, Switzerland, Paper (No. 1093).

Magenes, G., Penna, A., Senaldi, I. E., Rota, M. & Galasco, A. 2014. Shaking Table Test of a Strengthened Full-Scale Stone Masonry Building with Flexible Diaphragms. *International Journal of Architectural Heritage* 8(3): 349-375.

Papanicolaou, C.G., Triantafillou, T.C., Papathanasiou, M. & Karlos, K. 2008. Textile reinforced mortar (TRM) versus FRP as strengthening material of URM walls: out-of-plane cyclic loading. *Materials and Structures* 41:143–157.

Penazzi, D., Valluzzi, M. R., Saisi, A., Binda, L. & Modena, C. 2001. Repair and strengthening of historic masonry buildings in seismic areas. In *Proc. International congress, more than two thousand years in the history of architecture safeguarding the structure of our architectural heritage*, Bethlehem, Palestine (pp. 1-6).

Prota, A., Marcari, G., Fabbrocino, G., Manfredi, G. & Aldea, C. Experimental in-plane behavior of tuff masonry strengthened with cementitious matrix–grid composites *Journal of Composites for Construction* 10 (3): 223-233.

Roca, P. & Araiza, G. 2010. Shear response of brick masonry small assemblages strengthened with bonded FRP laminates for in-plane reinforcement. *Construction and Building Materials* 24(8): 1372-1384.

Tumialan, J. G., Micelli, F. & Nanni, A. 2001. Strengthening of masonry structures with FRP composites (pp. 21-23). University of Missouri, Rolla.

UNI EN 12390-3 2009. Testing hardened concrete, Part 3: Compressive strength of test specimens.

UNI EN 1926 2007. Natural stone test methods – Determination of uniaxial compressive strength.